*Reprinted from*

APPLIED PHYSICS EXPRESS

**Highly Stable Vortex State in Sub-100 nm Nanomagnets**

Xinghua Wang, Indra Purnama, Murapaka Chandra Sekhar, and Wen Siang Lew

Appl. Phys. Express **5** (2012) 053001

Applied Physics Express **5** (2012) 053001
DOI: 10.1143/APEX.5.053001

# Highly Stable Vortex State in Sub-100 nm Nanomagnets

Xinghua Wang, Indra Purnama, Murapaka Chandra Sekhar, and Wen Siang Lew*

*School of Physical and Mathematical Sciences, Nanyang Technological University, 21 Nanyang Link, Singapore 637371*

Received February 20, 2012; accepted March 26, 2012; published online April 12, 2012

We report on the magnetization reversal process in sub-100 nm $Ni_{80}Fe_{20}$ asymmetric ring. The switching mechanism involves a stable vortex state due to the strong anisotropy imposed on the narrow arm of the ring. Experimental demonstration shows that such vortex configuration does not annihilate until a large reversal field of 1200 Oe. The asymmetry of the structure promotes a unique reversal process, which gives us control over the chirality of the vortex configuration. Micromagnetic simulations reveal that the highly stable vortex configuration is sustainable in the asymmetric ring structures with a diameter as small as 30 nm. © 2012 The Japan Society of Applied Physics

Nanoscale magnetic circular disks[1,2] and rings[3–5] have been identified as potential recording elements for next-generation storage media due to the merits of simple and reproducible switching mechanisms.[6] The studies of size-dependent magnetic configuration and magnetic switching process in thin-film patterned disk structures have been well established. For instance, the magnetic configuration of a circular disk pattern is shown to change from a vortex state to a single-domain state when the diameter of the disk is reduced beyond a critical value.[7] When the lateral dimension is smaller than this critical value, the significant increase of the exchange energy will overshadow the magnetostatic energy, making the single-domain state more favorable energetically.[8] Towards achieving ultrahigh-density recording, the size of the magnetic elements[9] has to be shrunk to the sub-100 nm range. The size-dependent magnetic configuration can limit the disk applications as a recording element in magnetic memory devices. Removing the vortex core in the disk to create a ring pattern forms a ring vortex magnetic configuration, and the vortex state is found to be relatively more stable.[10–12] However, with the ring size reduction, two issues arise. First, the chirality of the vortex state is not controllable; it can be anticlockwise or clockwise. Second, the vortex state in the sub-100 nm rings is only stable in the field range less than 100 Oe. From the application viewpoint, the stability of the vortex state is critical for use as a recording medium.[13] Moreover, the ability to manipulate the vortex state with a determined chirality is also important. In the present work, we demonstrate a persistent vortex in the sub-100 nm asymmetric ring. The vortex state is highly stable with a reversal field of 1200 Oe. The magnetization on the narrow part of the nanoring does not rotate until a large reverse field is applied due to the strong shape anisotropy imposed on that area, giving us the large coercivity. Additionally, the chirality of the vortex state can be controlled via field history due to the imposed geometrical asymmetry. Micromagnetic simulations reveal that the controllable vortex state is sustainable in the asymmetric ring with a diameter as small as 30 nm.

Asymmetric ring-shaped $Ni_{80}Fe_{20}$ (NiFe) nanomagnets were fabricated using electron beam lithography and lift-off processes. Magnetron sputtering technique was used to grow Si/Ta (5 nm)/NiFe (8 nm)/Ta (5 nm) structures. The Ta films were used as buffer and protection layers for the NiFe. The sputtering pressure was maintained at 3.5 mTorr and the base pressure was better than $3.0 \times 10^{-8}$ Torr.

*E-mail address: wensiang@ntu.edu.sg

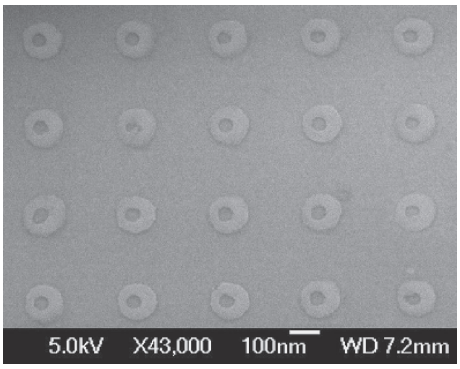


**Fig. 1.** Scanning electron microscopy image of an array of NiFe asymmetric rings. The outer diameter $D_o$ of the asymmetric ring is 100 nm, and the inner diameter $D_i$ is 50 nm.

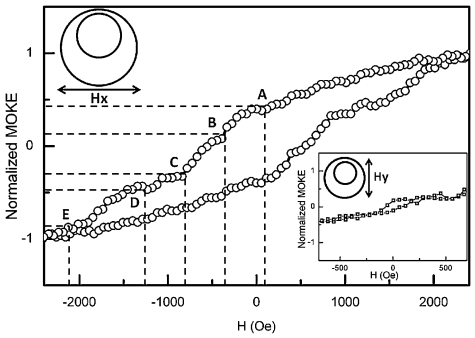


**Fig. 2.** Normalized MOKE hysteresis behavior measured on an array of NiFe asymmetric rings with fields applied along the $x$-axis and $y$-axis (inset).

Shown in Fig. 1(a) is a SEM image of an array of asymmetric ring-shaped nanomagnets. The outer diameter ($D_o$) of the fabricated ring structure is 100 nm while the inner diameter ($D_i = 0.5D_o$) is 50 nm. The asymmetry was induced by offsetting the center of the inner circle by a distance [$l$ ($= 0.1D_o$) of 10 nm], with respect to the center of the outer circle. The spacing between the rings was maintained at 200 nm. The asymmetry axis is defined as the $x$-axis while the symmetry axis is defined as the $y$-axis.

Shown in Fig. 2 is the normalized hysteresis loop of the NiFe asymmetric nanoring structure arrays measured by magneto-optical Kerr effect (MOKE) magnetometry at room temperature with fields applied along the $x$-axis. A multi jump hysteresis loop is obtained. As the field strength is reduced from $+x$ saturation, the magnetization decreases gradually

until a critical field of +100 Oe, corresponding to point A in the loop. The gradual decrease of the magnetization along the field direction is attributed to the change from single domain state, where all the magnetization is aligned to the field direction, to the onion state, where half of the magnetization rotates clockwise and the other half rotates counter-clockwise. On reversing the field to −300 Oe, the magnetization jumps rapidly corresponding to region AB in the loop. The observed magnetization jump is attributed to the movement of the transverse domain walls towards the narrow part of the asymmetric ring.[14] Since the domain wall energy[15,16] depends on the width of the ring arm, the narrow arm of the asymmetric ring forms an energy well for the domain walls. Consequently, all the domain walls nucleated during the switching process move to the narrow arm of the asymmetric ring. On further increasing the magnetic field in the negative direction, the magnetization gains monotonically in the field region −300 to −700 Oe, which is marked as region BC. Following that, the magnetization shows a plateau like condition (region CD), indicating that a stable state is present in the asymmetric nanoring. This plateau like region signifies the formation of a vortex configuration, where the magnetization vectors align along the edge of the structure. As the field is further increased in the $-x$-direction, a jump in magnetization that leads to negative saturation (E) is observed.

When the magnetic field is applied along the $y$-direction, a single switch hysteresis loop is obtained as shown in the inset of Fig. 2. As the field is reduced from positive saturation to −50 Oe, a switch in the magnetization occurs. When the field is swept from negative saturation to positive saturation, the magnetization switches at −50 Oe. The switch at the relatively low field produces a near-square loop. This is an indication of a coherent rotation of the spins.[17] As the field is reduced from the total saturation state, the spin is expected to align along the ring shape, i.e., an onion configuration. Hence, the magnetization changes from onion to reverse onion, without having any intermediate state. The MOKE measurement produces a relatively low signal-to-noise ratio; however, the different behaviors of the two reversal processes can still be distinguished from the large coercvity that is only found when the magnetic field is applied along the $x$-axis.

In order to aid our understanding of the reversal process in the sub-100 nm asymmetric ring, micromagnetic simulations were carried out with the field conditions corresponding to those in Figs. 2(a) and 2(b). The magnetization configurations and switching properties were obtained by using the OOMMF[18] simulation program. The intrinsic parameters for NiFe were used in the simulation: crystalline anisotropy constant $K_1 = 0$, saturation magnetization $M_s = 8.6 \times 10^5$ A m$^{-1}$, exchange stiffness $A = 1.3 \times 10^{-11}$ J m$^{-1}$, and damping coefficient $\alpha = 0.5$. To model the reversal process for fields applied along the $y$-direction, a large field of 6000 Oe was applied along the $+y$-direction to saturate the magnetization. When the field is decreased close to +300 Oe, a positive onion spin configuration is formed, with two domain walls nucleated at the symmetric axis and the spins align along the ring shape. Upon reducing the field, the magnetization gradually decreases and then switches abruptly at a field close to zero. The magnetization then progressively increases as the field is increased in the negative direction and reaches negative saturation. The simulated spin configurations confirm our interpretation of the MOKE measurement that the asymmetric ring structure adopts a switching process where all the spins rotate coherently from the configurations of negative onion to positive onion without going through intermediate states.

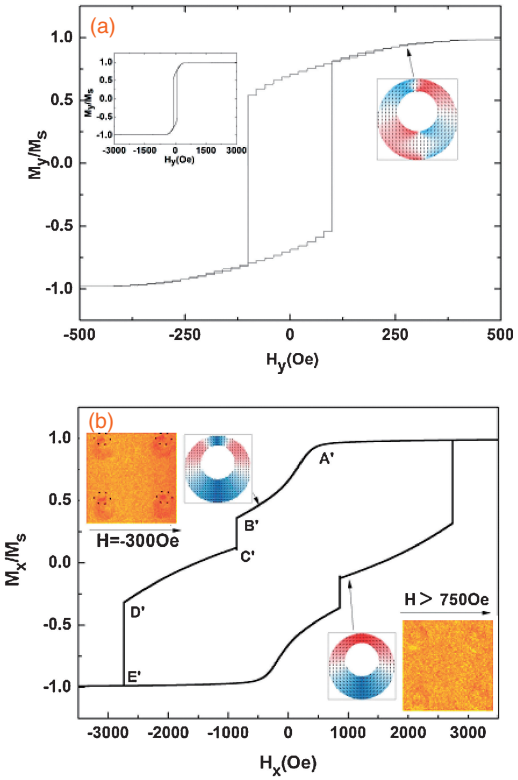


**Fig. 3.** Simulated hysteresis loops of NiFe asymmetric rings ($D_o = 100$ nm, $t = 8$ nm) and their spin configurations (insets). (a) A near-square loop indicates a spin switching via coherent rotation when the field is applied along the $y$-axis. A fully saturated loop is shown in the inset. (b) A multi jump loop indicates a spin switching via the formation of a vortex state when the field is applied along the $x$-axis. Insets are MFM images scanned with in an situ magnetic field. The dotted circles are inserted for reading guidance.

The simulated $M$–$H$ loop for fields applied along the $x$-axis is shown in Fig. 3(b). When the field is reduced, a significant decrease in magnetization is observed, spreading a field distribution of around 300 Oe (A′B′). This is followed by an abrupt magnetization drop (B′C′) at a critical field of −1000 Oe. Our simulated magnetic configurations have revealed that the magnetization drop in the A′B′ region is due to the movement of two transverse domain walls. The transverse domain walls are nucleated at asymmetric axis forming the onion state, and move to the narrow part of the asymmetric ring to form a 360° domain wall. The B′C′ abrupt switch is caused by the annihilation of the 360° domain wall leading to a vortex state. On the other hand, the spin orientation of the wide arm remains unchanged, aligning to the $+x$-direction. The interesting feature of this finding is that the chirality of the vortex state, which is determined by the spin orientation of the wide arm, can be decided on the basis of the saturation field direction, in contrast to the case of the symmetric rings. On increasing the negative field, the magnetization reaches a quasi-stable plateau of C′D′, and then another switch at E′. The switch at D′E′ is attributed to the reversal of magnetization at the wide arm of the

asymmetric ring. The C′D′ plateau region extends more than 1500 Oe and the simulated spin configurations show that a stable vortex state is present. Thus, the switching process is a transition from an onion to a reverse onion state via the formation of the vortex state. The measured MOKE hysteresis loops are qualitatively confirmed from the simulation. Some minor differences such as the simulated coercivity and saturation field are relatively larger than the measured values. These are possibly attributable to thermal fluctuations and switching field distribution. As the thermal fluctuation is not taken into consideration in the micromagnetic simulation, the switching fields tend to be overestimated. The broadening of the switching field in the BC region and the slanted measured loops are due to the distribution of the switching fields in the measured asymmetric nanoring samples.

In order to observe the magnetic configurations directly at the above-mentioned regions, magnetic force microscopy (MFM) scanning with *in situ* magnetic field was carried out. The MFM images are shown in the insets of Figs. 3(a) and 3(b). A lift-scan-height of 50 nm was used for all the scanning. A large magnetic field of −3000 Oe was initially applied along the *y*- or *x*-axis to magnetically saturate the asymmetric ring structures; the field was then reduced to −300 Oe to induce a magnetic state. When the field is in the *y*-axis direction (symmetric axis), the MFM image shows that an onion state with a domain wall at the narrow and wide arms was obtained. When the field is applied along the *x*-axis (asymmetric axis), a relatively low contrast MFM image with a black region in the narrow arm was obtained, which is corresponding to the domain wall at the narrow arm. When the field is increased above +750 Oe, a lower contrast MFM image indicating a vortex state was obtained. The MFM results confirm that the plateau in our MOKE hysteresis loop was due to the formation of the vortex state.

To further investigate the magnetic configuration at smaller scales, systematic simulations were carried out on asymmetric nanorings of different sizes ($D_o = 30$, 50, and 70 nm, $D_i = 0.5D_o$ and $l = 0.1D_o$). The chosen thicknesses $t$ are 8, 12, and 16 nm. A representative of simulated hysteresis loops of the ring structures as a function of $D_o$ and $t$ is shown in Fig. 4. The results can be categorized into single-switched and double-switched hysteresis loops. The double-switched loop, which corresponds to the switching process via the formation of a vortex state, is observed in rings with thickness larger than 12 nm and a lateral size as small as 30 nm. The single-switched loop is shown in 8- and 12-nm-thick asymmetric rings of 30 nm $D_o$, showing single-domain characteristics. Moreover, the saturation field of the double-switched loop is much larger than that of the single-switched loop. These two different switching properties shown are mainly due to two reasons. First, in the larger ($D_o > 30$ nm) and thicker ($t > 12$ nm) asymmetric rings, the introduction of asymmetry into the ring structure has caused the configuration stability of the formed onion state to be smaller than that in the symmetric ring. Second, the domain wall energy well in the narrow arm has induced a selective movement of the domain walls of the onion state, rendering the vortex state more favorable. When the lateral size and film thickness in the asymmetric ring shrink further ($D_o < 30$ nm, $t < 12$ nm), the significant increase of the exchange energy renders the vortex state unfavorable.

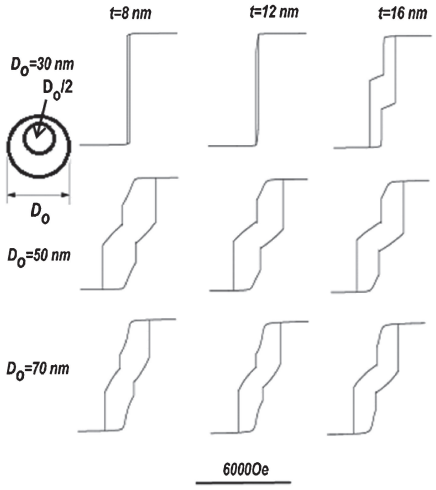


**Fig. 4.** Hysteresis loops simulated as a function of diameter and thickness of the NiFe asymmetric ring. For each loop, the horizontal axis is the applied field and the vertical axis is the normalized magnetization. The field is applied along the *x*-axis. The results show that the vortex state remains in the asymmetric ring with a diameter as small as 30 nm.

In summary, combining MOKE measurement, micromagnetic simulations, and MFM scanning on sub-100 nm asymmetric rings, we have revealed that the switching process is field orientation dependent. When the external field is applied along the *y*-axis, the magnetization switches via a key process of onion-reverse onion with all the spins rotating coherently, whereas that of the *x*-axis, the magnetization switches via a process of onion-vortex-reverse onion. The observed intermediate vortex state is highly stable and the chirality of the vortex state is controllable. The vortex state is persistently existent even when the ring diameter approaches a small lateral dimension, i.e., 30 nm, which is smaller than the critical size of the disk pattern. The highly stable vortex state and its chirality control feature in the asymmetric ring have promising applications in magnetic recording devices.

**Acknowledgments** This work was supported in part by the ASTAR SERC grant (082 101 0015) and the NRF-CRP program (Multifunctional Spintronic Materials and Devices). We would also like to thank J. Deng and S. L. Teo from the Institute of Materials Research and Engineering for the help in the sample fabrication, and S. Goolaup from the University of Mauritius for the helpful discussions.

1) C. A. Ross: Annu. Rev. Mater. Res. **31** (2001) 203.
2) T. Taniuchi *et al.*: J. Electron Spectrosc. Relat. Phenom. **144** (2005) 741.
3) M. Kläui *et al.*: J. Phys.: Condens. Matter **15** (2003) R985.
4) C. A. Ross *et al.*: J. Appl. Phys. **99** (2006) 08S501.
5) Y. G. Yoo *et al.*: Appl. Phys. Lett. **82** (2003) 2470.
6) J. Rothman *et al.*: Phys. Rev. Lett. **86** (2001) 1098.
7) K. Y. Guslienko *et al.*: Phys. Rev. Lett. **100** (2008) 027203.
8) C. A. F. Vaz *et al.*: J. Phys.: Condens. Matter **19** (2007) 255207.
9) M. Heumann *et al.*: Phys. Rev. Lett. **94** (2005) 077202.
10) L. J. Heyderman *et al.*: Microelectron. Eng. **73–74** (2004) 780.
11) M. Kläui *et al.*: J. Magn. Magn. Mater. **272–276** (2004) 1631.
12) S. P. Li *et al.*: J. Appl. Phys. **92** (2002) 7397.
13) J. K. Ha *et al.*: Phys. Rev. B **67** (2003) 064418.
14) X. H. Wang *et al.*: J. Appl. Phys. **106** (2009) 043905.
15) F. Q. Zhu *et al.*: Phys. Rev. Lett. **96** (2006) 027205.
16) X. H. Wang *et al.*: Appl. Phys. Lett. **97** (2010) 142504.
17) W. S. Lew *et al.*: J. Appl. Phys. **87** (2000) 5947.
18) M. J. Donahue and D. G. Porter: OOMMF User's Guide, Version 1.0 Interagency Report NISTIR 6376, National Institute of Standards and Technology, Gaithersburg, MD, 1999.